J. Membrane Biol. 161, 9–19 (1998)

The Journal of
Membrane
Biology

Effects of Lens Major Intrinsic Protein on Glycerol Permeability and Metabolism

C. Kushmerick, K. Varadaraj, R.T. Mathias

Department of Physiology and Biophysics, State University of New York at Stony Brook, Stony Brook, New York 11794-8661, USA

Received: 23 May 1997/Revised: 4 August 1997

Abstract. Lens Major Intrinsic Protein (MIP) is a member of a family of membrane transport proteins including the Aquaporins and bacterial glycerol transporters. When expressed in *Xenopus* oocytes, MIP increased both glycerol permeability and the activity of glycerol kinase. Glycerol permeability (p_{Gly}) was $2.3 \pm 0.23 \times 10^{-6}$ cm sec^{-1} with MIP *vs.* $0.92 \pm 0.086 \times 10^{-6}$ cm sec^{-1} in control oocytes. The p_{Gly} of MIP was independent of concentration from 5×10^{-5} to 5×10^{-2} M, had a low temperature dependence, and was inhibited approximately 90%, 80% and 50% by 1.0 mM Hg^{++}, 0.2 mM DIDS (diisothiocyanodisulfonic stilbene), and 0.1 mM Cu^{++}, respectively. MIP-enhanced glycerol phosphorylation, resulting in increased incorporation of glycerol into lipids. This could arise from an increase in the total activity of glycerol kinase, or from an increase in its affinity for glycerol. Based on methods we present to distinguish these mechanisms, MIP increased the maximum rate of phosphorylation by glycerol kinase (0.12 ± 0.03 *vs.* 0.06 ± 0.01 pmol min^{-1} $cell^{-1}$) without changing the binding of glycerol to the kinase ($K_M \sim 10$ μM).

Key words: MIP26 — Lens fiber cell — Glycerol — Cell membrane permeability — Glycerol kinase

Abbreviations: DIDS, diisothiocyanodisulfonic stilbene; G3P, α-glycerol-3-phosphate; GK, Glycerol Kinase EC 2.7.1.30; MIP, Major Intrinsic Protein of Lens

Introduction

Lens Major Intrinsic Protein (MIP) is the most abundant membrane protein in the fiber cells of the ocular lens (Broekhuyse, Kuhlmann & Stols, 1976). MIP appears in equatorial epithelial cells as they differentiate to form new fiber cells, and thus it is found in differentiating and mature fiber cells but not in the epithelium that caps the anterior hemisphere. MIP is a 28 kDa intrinsic membrane protein, with an amino acid sequence predicted to span the plasma membrane six times (Gorin et al., 1984). Amino acid sequence comparison indicates it is a member of a superfamily of membrane transport proteins with similar sequence and predicted membrane topology (Baker & Saier, 1990), including the Aquaporin water channels (Agre et al., 1993) and the bacterial glycerol facilitators glpF and FPS1 (Maurel et al., 1994; Luyten et al., 1995). Therefore, it is likely lens MIP is also a membrane transport protein. However, glpF and FPS also affect glycerol metabolism (Voegele, Sweet & Boos, 1993; Luyten et al., 1995). This suggests proteins of the MIP superfamily, in general, may have a role in metabolism as well as membrane transport.

The role of MIP in the lens is poorly understood, however mutations in MIP underlie cataract development in mice, suggesting it is essential for lens homeostasis (Shiels & Bassnett, 1996). MIP was originally thought to form gap junctions between fiber cells, but this hypothesis is now considered unlikely. Based on sequence analysis, immunocytochemistry, and functional data, MIP neither resembles nor behaves like the connexin family of gap junction proteins, members of which are present in the lens (Beyer, Paul & Goodenough, 1987; Zampighi et al., 1989; Swenson et al., 1989). Reconstitution of MIP into artificial lipid bilayer systems demonstrated it can form ion channels with large (hundreds of pS) open channel conductances (Ehring et al., 1990) and nonspecific channels permeable to neutral solutes as large as sucrose (Girsch & Peracchia, 1985). However, when expressed in the plasma membrane of *Xenopus* oocytes, MIP does not cause a detectable increase in conductance but forms a channel for water and facilitates glycerol uptake (Kushmerick, et al., 1995; Mulders et al., 1995; Zampighi et al., 1995). The

Correspondence to: R.T. Mathias

inability of expressed MIP to transport ions may be representative of its behavior in the lens fiber cells, which have a very low conductance despite the fact that MIP is abundant (Mathias et al., 1985). In addition to increasing glycerol and water transport, expression of MIP generated a significant nonsaturable component of glycerol uptake (Kushmerick et al., 1995). This component was consistent with an increase in trapping of glycerol as impermeant metabolites, suggesting MIP may be involved in metabolism as well as membrane permeation of glycerol in the lens.

The purpose of this paper is to investigate the role of MIP in transport and metabolism of glycerol. As in most cells, the first step in glycerol metabolism is formation of glycerol-3-phosphate. We developed a method to determine free intracellular glycerol, allowing us to measure simultaneously the kinetics of glycerol uptake and phosphorylation in the oocyte.

When extracellular glycerol is in the millimolar range, we show its influx into oocytes is much greater (~100-fold) than its rate of disappearance by metabolism. Thus, virtually all ^{3}H-glycerol taken up remains as free glycerol, and radioactive uptake is a direct measure of permeability. Under these conditions, we characterized the concentration dependence, heavy metal sensitivity and temperature sensitivity of the glycerol permeability of MIP.

Materials and Methods

Expression of MIP in *Xenopus* Oocytes

Synthesis of mRNA, isolation and injection of oocytes, production of anti-MIP antisera and quantifying of expression by Western blotting using purified frog lens MIP for calibration were performed exactly as previously described (Kushmerick et al., 1995). In brief, capped mRNA with a frog viral promoter and a poly-A tail was prepared from a frog (*Rana pipiens*) MIP cDNA clone (Austin et al., 1990) using the MEGAscript (Ambion, Austin, TX) *in vitro* translation kit. Oocyte Ringer solution contained (in mM): NaCl (82.5), KCl (2.5), $CaCl_2$ (1), $MgCl_2$ (1), Hepes (5), pH 7.8, penicillin and streptomycin, 10 μg ml^{-1} each. Oocytes were isolated from *Xenopus leavis* and defolliculated using collagenase (Sigma Type XIII, 120 min, 2 mg ml^{-1} in Ca^{2+}-free Ringer). After isolation, oocytes were incubated overnight at 18°C. They were then injected with either 50 nl of a solution containing 0.2 g l^{-1} (10 ng) synthetic MIP mRNA or 50 nl H_2O (controls). After injection, oocytes were incubated for 72 hr at 18°C prior to experimentation. Expression was quantitated by Western blotting using polyclonal anti-peptide rabbit antiserum raised against the final 19 amino acids of frog MIP and the ECL western blotting detection reagents.

Measurement of ^{3}H-glycerol Uptake

Individual oocytes were incubated in 0.5 ml Ringer solution containing 1 μCi/ml ^{3}H-glycerol (72 Ci mmol^{-1}, NEN, Boston, MA), and unlabeled glycerol to give the final concentration indicated in the text. When uptake was measured in the presence of inhibitors ($HgCl_2$, DIDS or $CuCl_2$), the oocytes were preincubated with the inhibitor for 10 min prior to the start of uptake. To stop the uptake reaction, oocytes were transferred using a wide-bore plastic transfer pipette to 7 ml plastic scintillation vials filled with ice-cold Ringer solution. The solution was removed from the vial by aspiration, and the vial was refilled from a supply of Ringers solution kept on ice. The oocytes were washed in this manner 4 times with a total of 28-ml Ringers solution within 30 sec. After the final wash was withdrawn, 0.5 ml 1% SDS was added and the oocytes were incubated for 30 min with occasional agitation until the oocyte dispersed in the detergent solution. Lastly, 3 ml of scintillation fluid was added to the tube (Ecolite$^+$, ICN, Costa Mesa, CA) and radioactivity counted. Each uptake measurement reported is the mean of 5–8 oocytes assayed independently. Thus a slope derived from three time points represent data from 15–24 oocytes, each assayed independently. Scintillation counter background, and background corresponding to nonspecific binding of glycerol to the oocyte (determined from the y-axis intercept of regression lines through 3–4 time points at t < 30 min) were subtracted from uptake values used to determine initial slopes.

Analysis of ^{3}H-glycerol Metabolites

Oocytes incubated in ^{3}H-glycerol were separated into their lipid and water-soluble components according to the method of Bligh and Dyer as described in Kates, 1986. The lipid fraction was separated into classes by thin-layer chromatography (TLC; silica-G / hexanes [bp ~69°C]:ethyl ether:glacial acetic acid::80:20:1). Monoglycerides were separated from phospholipids using the solvent system: $CHCl_3$:MeOH:H_2O::64:25:4. Lipid classes were identified based on their mobility in comparison to lipid standards (Sigma). The water soluble fraction was separated by TLC (silica-G / isopropanol: water: MH_3OH::70:20:10). ^{3}H-G3P, used for a standard, was synthesized by incubating ^{3}H-glycerol with glycerol kinase (Boehringer Mannheim, Indianapolis, IN) in a buffer containing (in mM): Tris HCl pH 8.0 (50), KCL (50), ATP (5), $MgCl_2$ (10), DTT(7.5). To quantify the TLC of radiolabeled metabolites, we used plastic-backed TLC plates (Macherey-Nagel, Germany), which were cut into 1 × 4-cm rectangles, placed in scintillation vials, stirred for 30 min with 7 ml scintillation fluid and counted.

Measurement of Oocyte Water Permeability

Oocyte volume change was monitored by video microscopy during hypotonic challenge as described (Kushmerick et al., 1995). Total oocyte water permeability (cm^3 sec^{-1}) was defined as

$$P_{H2O} = \frac{dV/dt}{V_{H2O}\,\Delta c}$$

where $V(t)$ is the oocyte volume, V_{H2O} = 18.2 cm^3 mol^{-1} is the molar volume of water and Δc is the imposed osmotic gradient.

Curve Fitting

All curve fitting was performed using the Marquardt-Levenson algorithm, as implemented in the software SigmaPlot (Jandel Corp.). The theory lines in Fig. 1 were the best-fit curves based on Eq. 8 in ref (Kushmerick et al., 1995). The theory lines in Fig. 6 were best-fit curves based on the equation

$$P_{Gly} = k_a\, e^{k_b/T}$$

The curves were used to interpolate the data points to calculate Q_{10} around 22°C.

Statistics

Unless otherwise stated, values are reported as mean ± SD. Values of slopes are given as least-squares regression slope ± slope SD.

List of Symbols

A_M	Area of oocyte plasma membrane (cm^2)
GK	Intracellular glycerol kinase (M)
GKC	Intracellular glycerol-glycerol kinase complex (M)
GKC_{ss}	Steady-state intracellular glycerol-glycerol kinase complex (M)
Gly_o	Extracellular glycerol (M)
Gly_i	Intracellular glycerol (M)
$Gly_{i\text{-}ss}$	Steady-state intracellular glycerol (M)
$G3P$	Intracellular glycerol-3-phosphate (M)
α	Forward rate constant for formation of glycerol-glycerol kinase complex(M^{-1} sec^{-1})
β	Dissociation rate constant for glycerol-glycerol kinase complex (sec^{-1})
k_p	Rate constant for formation of G3P from GKC (sec^{-1})
K_M	Apparent Michaelis constant of GK for glycerol (M)
k_{mem}	Membrane rate constant for glycerol (sec^{-1}) ($=S_i/\mathrm{Gly}_o v_{\mathrm{Gly}}$)
p_{Gly}	Specific membrane permeability for glycerol (cm sec^{-1}) ($=S_i/Gly_o A_M$)
P_{Gly}	Total oocyte permeability for glycerol ($cm^3 sec^{-1}$) ($=S_i/Gly_o$)
P_{H2O}	Total oocyte permeability for water (cm^3 sec^{-1})
$Q_{10}(T)$	Ratio of reaction rate at (T + 5)°C to (T − 5)°C
S_f	Final slope of glycerol uptake (mol min^{-1})
S_i	Initial slope of glycerol uptake (mol min^{-1})
V_{Gly}	Glycerol-accessible volume (cm^3)

Results

Glycerol Uptake Time Course

Figure 1 shows the time course of glycerol uptake into oocytes expressing MIP or control oocytes. Oocytes were incubated in 20 μM ^{3}H-glycerol for the indicated times, then intracellular ^{3}H-radioactivity (including glycerol and its metabolites) determined by scintillation counting. After an initial linear phase (t < ~30 min) and a transitional phase, uptake entered a final linear phase (t > ~200 min), which lasted for at least 1420 min. Expression of MIP increased both the initial slope (S_i; MIP: 0.15 ± 0.04 *vs.* Control: 0.06 ± 0.01 pmol min^{-1}) and the final slope (S_f; MIP: 0.035 ± 0.0029 *vs*. Control: 0.014 ± 0.0007 pmol min^{-1}).

Given an oocyte glycerol volume of ~0.75 μl (*see below*), oocytes will contain 15 pmol of free glycerol when at equilibrium with 20-μM glycerol in the bath. As seen in Fig. 1, both control oocytes and oocytes expressing MIP accumulated glycerol beyond equilibrium. Simple diffusion of glycerol into the cell cannot explain this observation. Since we found no evidence of active transport of glycerol by oocytes expressing MIP or control oocytes (Kushmerick et al., 1995), we hypothesize glycerol kinase trapped it in the cell and allowed it to accumulate.

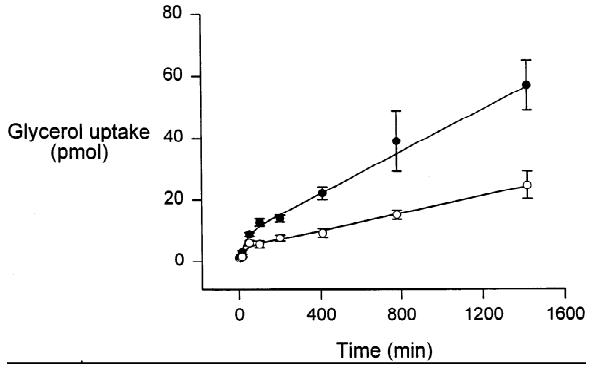

Fig. 1. Time course of glycerol uptake in oocytes expressing MIP (●) or control oocytes (○). Oocytes were incubated in 20 μM ^{3}H-glycerol for the times indicated, then washed and counted as described in Materials and Methods. Total oocyte radioactivity was measured, which includes free glycerol and its cellular metabolites. Each point is the mean of 6 oocytes assayed independently. Error bars are standard errors of the mean. Smooth lines were generated by an equation representing the reaction in Eq. 1.

Chemical Basis of the Final Slope, S_f

Accumulation of metabolites of glycerol could explain the continuous uptake of ^{3}H-glycerol beyond equilibrium. Figure 2 shows an overview of glycerol handling in the liver (Lin, 1977). The first step is phosphorylation to glycerol-3-phosphate (G3P) followed by incorporation into lipid. G3P may also enter glycolysis after conversion to DHAP, however note that in physiologic conditions, [DHAP]/[G3P] < 10^{-4} (based on data in Bergmeyer, 1984 and Klaidman, Leung & Adams, 1995, assuming pH ≃ 7.0).

To determine which pathway(s) are involved in metabolism of glycerol in oocytes, we performed thin-layer chromatography on the aqueous and lipid fractions of oocytes incubated for 18 hr in 20-μM ^{3}H-glycerol. This time point and concentration was chosen to maximize components other than free glycerol and thus make their detection easier.

Table 1 lists the radiolabeled chemical forms we identified and their relative abundances. Consistent with metabolic trapping, a large portion of the water-soluble radioactivity was identified as glycerol-3-phosphate. The major lipid forms were phospholipids, with smaller contributions from mono-, di- and tri-glycerides. Thus the oocyte, like other cell types (Lin, 1977), incorporates

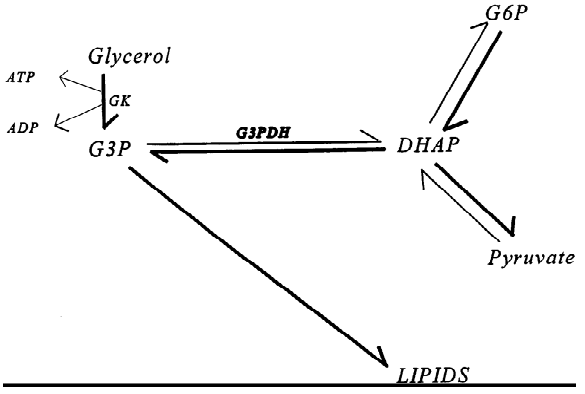

Fig. 2. Overview of glycerol handling in the liver based on data in Lin (1977). The first step is phosphorylation, followed by incorporation into lipid or conversion into DHAP for entry into glycolysis. Note that under typical cellular conditions, intraconversion of G3P and DHAP strongly favors formation of G3P. Abbreviations are: DHAP, dihydroxyacetone phosphate; G3P, glycerol-3-phosphate; G3PDH, glycerol-3-phosphate dehydrogenase; G6P, glucose-6-phosphate; GK, glycerol kinase.

Table 1. Oocyte expressing frog MIP lipid fraction on TLC

Fraction	Chemical form	% of Fraction	% of total
Water soluble	Glycerol	29	14.5
	Glycerol-3-phosphate	58	29
	Unidentified	13	6.5
Lipid	Phospholipids	60	30
	Monoglycerides	2	2
	Diglycerides	18	9
	Triglycerides	18	9

Oocytes were incubated in 20 μM ^{3}H-glycerol for 18 hr, then separated into lipid and water-soluble fraction by the method of Bligh and Dyer (described in Kates, 1986). The lipid fraction was separated into classes by TLC and the percentage of ^{3}H-labeled lipid for each class measured. The water-soluble fraction was separated by TLC and the fraction ^{3}H-glycerol and ^{3}H-G3P measured. Glycerol and G3P were determined by comparison of their mobility with authentic ^{3}H-glycerol and ^{3}H-G3P, the latter synthesized as described in Materials and Methods. Lipid classes were identified by comparison with lipid standards (Sigma) as follows: Phospholipids: egg phosphatidylcholine and phosphatidylethanolamine; Monoglycerides: 1-monolinoleoyl-rac-glycerol; Diglycerides: 1,3-dilinolein; triglycerides: trilinolein. Lipid standards were visualized by staining with I_2.

glycerol into lipid and metabolic trapping explains the uptake of glycerol beyond equilibrium.

Model Calculations

Following the observation that the *E. coli* glycerol facilitator, which is a member of the MIP superfamily, enhances the activity of glycerol kinase (Voegele et al., 1993), we hypothesize MIP activates glycerol kinase in the oocyte. We assume glycerol enters the cell passively, followed by phosphorylation by glycerol kinase. The most simple representation is:

$$Gly_o \underset{k_{\mathrm{mem}}}{\overset{k_{\mathrm{mem}}}{\rightleftharpoons}} Gly_i + GK \underset{\beta}{\overset{\alpha}{\rightleftharpoons}} GKC \xrightarrow{k_p} G3P + GK \qquad (1)$$

Where Gly_o is the extracellular (bath) glycerol concentration and Gly_i, *GK*, *GKC* and *G3P* are the intracellular glycerol, glycerol kinase, glycerol-glycerol kinase complex and glycerol-3-phosphate concentrations, respectively. Table 1 shows *G3P* is incorporated into lipid. However, our data represent *G3P* and all of its impermeant products and insofar as the formation of *G3P* is irreversible, downstream reactions do not affect our analysis (*see* Discussion). *G3P* may also be converted to dihydroxyacetone phosphate and enter the glycolytic pathway, resulting in loss of radioactivity as $^3H\text{-}H_2O$. As described in the Discussion, when this pathway is significant, accumulation of *G3P* (and products) begins to slow, hence the final slope is not linear. Since we are recording the linear phase of accumulation, we assume loss of radioactivity as $^3H\text{-}H_2O$ is negligible.

Equation 1 comprises the following reactions: the passive membrane permeation of glycerol into the cell, with equal forward and reverse rate constant, k_{mem} (sec^{-1}); the reversible association of glycerol with glycerol kinase with forward rate α (M^{-1} sec^{-1}) and reverse rate β (sec^{-1}); and the irreversible formation of G3P with rate constant k_p (sec^{-1}). α, β *and* k_p combine to form the Michaelis constant, $K_M = (\beta + k_p)/\alpha$, (M). The time dependence of the reactions in Eq. 1 follow from the definition of the rate constants:

$$\frac{d\,Gly_i}{dt} = k_{\mathrm{mem}}(Gly_o - Gly_i) - \alpha\, GK\, Gly_i + \beta\, GKC \quad \text{(a)}$$

$$\frac{d\,GKC}{dt} = \alpha\, GK\, Gly_i - (\beta + k_p)\, GKC \quad \text{(b)}$$

$$\frac{d\,G3P}{dt} = k_p\, GKC \quad \text{(c)} \qquad (2)$$

At early times, $Gly_i \sim 0$, and thus the initial slope of glycerol uptake, S_i (mol sec^{-1}), is given by

$$S_i = Gly_o\, k_{\mathrm{mem}}\, V_{Gly} \qquad (3)$$

Where V_{Gly} is the volume of the oocyte available to glycerol, (~0.75 μl; *see below*).

When uptake enters the slow linear phase (after about 200 min, *cf.* Fig. 1), Gly_i and *GKC* are at their steady state values, Gly_{i-ss} and GKC_{ss}, respectively. The final slope, S_f (mol sec^{-1}) is therefore given by:

$$S_f = k_p\, V_{Gly}\, GKC_{ss} = k_p\, V_{Gly}\, GK_T \frac{Gly_{i-ss}}{Gly_{i-ss} + K_M} \quad (4)$$

Where GK_T(M) is the total concentration of glycerol kinase present in the cell, comprising free and complexed enzyme.

At steady-state, the rate of entry of glycerol equals the rate of formation of *G3P* (i.e., the final slope, S_f). Thus we may write

$$S_f = k_{\text{mem}} V_{Gly}(Gly_o - Gly_{i-ss}) \quad (5)$$

Combining Eqs. 3 and 5 and solving for Gly_{i-ss} results in:

$$Gly_{i-ss} = Gly_o \left(1 - \frac{S_f}{S_i}\right) \quad (6)$$

In Eq. 6, the steady-state intracellular glycerol concentration is shown as a function of three experimental parameters: extracellular glycerol, and the initial and final slopes of uptake.

The parameters in Eq. 1 can be determined as follows: k_{mem} can be calculated from S_i and V_{Gly} using Eq. 3; K_M and $k_pGK_TV_{Gly}$ can be determined by fitting Eq. 4 to values of S_f *vs.* Gly_{i-ss} (Gly_{i-ss} having been calculated from Eq. 6); V_{Gly} is determined as described below.

Determination of V_{Gly}, the Glycerol-accessible Volume in the Oocyte

Calculations of intracellular concentrations and the membrane rate constant for glycerol require knowledge of the oocyte glycerol-accessible volume, V_{Gly}. To determine V_{Gly}, we incubated oocytes in 2.0 mM ^{3}H-glycerol. This concentration was chosen to be sufficiently high that metabolized glycerol is a negligible fraction of Gly_i, without imposing significant osmotic stress. After 400 min, further uptake was negligible (<0.6% hr^{-1}) indicating Gly_o and Gly_i were essentially at equilibrium. At equilibrium, oocytes took up 1500 ± 91 pmol ^{3}H-glycerol from a bath concentration of 2,000 pmol μl^{-1}, indicating free glycerol equilibrated with a volume of ~0.75 μl. In comparison, the oocyte volume for water has been estimated to be ~0.9 μl (Whitesell et al., 1993).

Effect of MIP on Glycerol Kinase

MIP could increase the activity of glycerol kinase in two ways: it could increase the affinity of the enzyme for glycerol (i.e., reduce K_M) or it could increase the maximum rate of phosphorylation (k_pGK_T). To distinguish these, we designed the following experiment. First, we measured the initial and final slope (S_i and S_f) of glycerol uptake at different extracellular glycerol concentrations (Fig. 3 *A* and *B*). Next, for each extracellular glycerol concentration, Gly_{i-ss} was calculated using Eq. 6. Finally, Eq. 4 was fit to our data on S_f *vs.* Gly_{i-ss} to determine K_M and k_pGK_T (Fig. 3*C*).

Table 2 summarizes the results from this analysis. The value of K_M was essentially unchanged for oocytes expressing MIP *vs.* Controls (~10 μM). The value of k_pGK_T, however, was increased by a factor of 2.3. Thus MIP increased the maximum rate of glycerol phosphorylation by glycerol kinase and not its affinity. Based on the initial slope data (Fig. 3*A*) k_{mem} (a measure of glycerol permeability) was increased by a factor of 2.1 by expression of MIP, as discussed in the following section.

We attempted to separately determine k_p and GK_T from our data, however our estimate of GK_T did not have sufficient resolution. *E. coli* glycerol kinase has a value of k_p on the order of 1,000 min^{-1} (calculated from data in Voegele et al., 1993). Using this value of k_p, GK_T in these oocytes is on the order of 100 pM whereas, Gly_i in these experiments ranges from 2 to 80 μM. Such a relatively small concentration of GK_T could not be determined by analysis of the kinetics of glycerol uptake and phosphorylation (if GK_T were on the order of Gly_i, it can be shown that GK_T can be estimated by extrapolating the final slopes back to $t = 0$. Therefore, we were unable to distinguish which of the terms in the maximum rate of phosphorylation, k_p or GK_T, is increased by MIP.

The effect of MIP on glycerol kinase was measured in 5 experiments using oocytes from different toads, at different times of the year and with different batches of MIP mRNA. Overall, expression of MIP increased k_pGK_T by a factor of 2.4 ± 0.5 (mean ± SD) relative to water-injected controls. A similar increase in k_pGK_T was seen when oocytes expressing MIP were compared to uninjected (rather than water-injected) controls. In the Discussion, we consider several alternative mechanisms for the effect of MIP on glycerol handling by the oocyte. We conclude the most likely interpretation of our data is also the most simple one: irreversible formation of *G3P* sets the final slope and the effect of MIP is to directly stimulate activity of glycerol kinase.

Effect of MIP on p_{Gly}

The specific permeability of the oocyte membrane to glycerol (p_{Gly}) was obtained from the initial slope of glycerol uptake (S_i), the external concentration (Gly_o) and the oocyte plasma membrane surface area (A_M) as:

$$P_{Gly} = \frac{S_i}{Gly_o A_M} \quad (7)$$

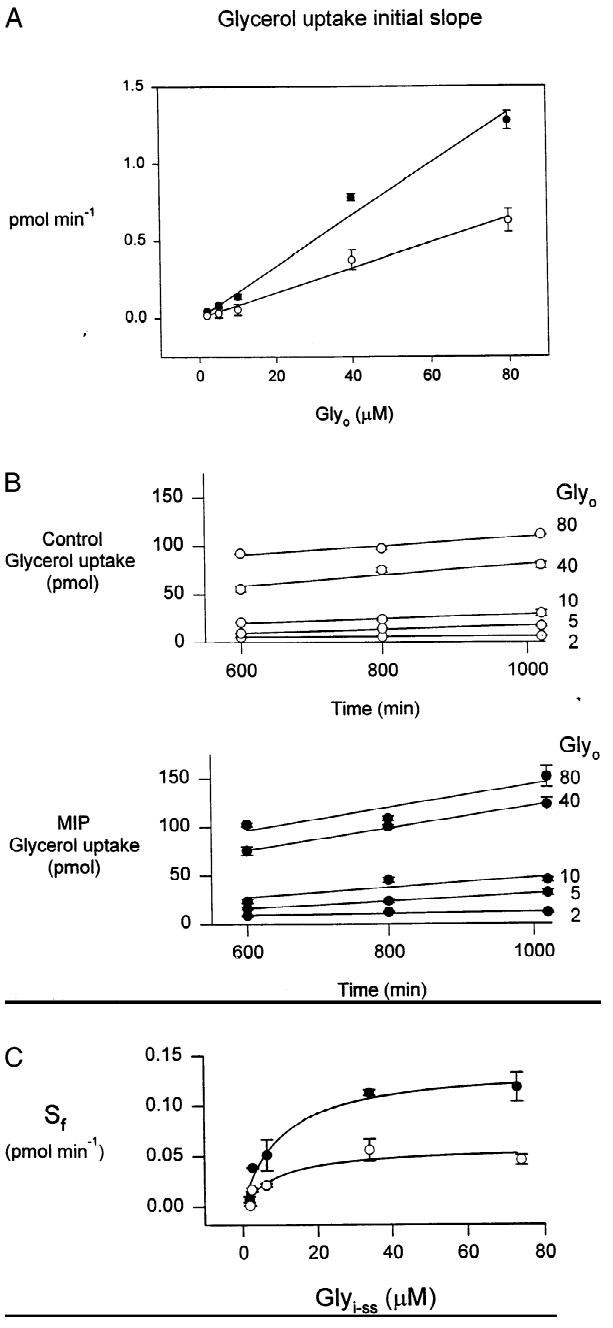

Fig. 3. Determination of model parameters. (*A*) The initial slope of glycerol uptake, S_i, was measured at different concentrations of Gly_o (2, 5, 10, 40, 80 μM) in oocytes expressing MIP (●) or control oocytes (○). Data points are means of 5–6 oocytes, error bars are standard deviations. (*B*) The final slope of uptake, S_f, was measured at different concentrations of Gly_o (2, 5, 10, 40, 80 μM) in oocytes expressing MIP (●) or control oocytes (○). Data points are means of 5–6 oocytes, error bars are standard errors of the mean. (*C*) Values of S_f (from the regression slopes in Fig. 3*B*) were plotted *vs.* the calculated free intracellular glycerol concentration determined from the initial and final slopes at each concentration. Eq. 4 (solid lines) was fit to the data using the Marquardt-Levenson algorithm. Parameters thus determined are presented in Table 2. Points are regression slopes from the data in panel *A*, error bars are regression slope standard deviations.

Table 2. Kinetic parameters for the uptake and metabolism of glycerol in oocytes

	k_{mem} ($\times 10^4$ sec)	K_M (μM)	$k_p\, GK_T\, V_{Gly}$ (pmol sec^{-1})
Control	1.8 ± 0.4	11.7	0.06 ± 0.013
MIP	3.8 ± 0.3*	12.5	0.12 ± 0.025*

* Difference (MIP *vs.* Control) is statistically significant ($P < 0.001$, by *t*-test). Equation 4 was fit to the data in Fig. 3 and Marquardt-Levenson curve-fitting used to determined the parameters k_{mem}, K_M and $k_p\, GK_T V_{Gly}$.

Data in Fig. 3*A* show MIP imparts a 2.1-fold increase in the initial slope of glycerol uptake which is linearly dependent on extracellular glycerol concentration from 2–80 μM. Figure 4 extends this result from 0.05 to 100 mM. Over this range, the initial uptake in both control and MIP-expressing oocytes exhibited a linear dependence on glycerol concentration, with MIP imparting a 2.5-fold increase in uptake rate. Thus over this range of glycerol concentrations, the glycerol permeability was constant and increased 2.5-fold by MIP. Linear regression was used to obtain a best-fit slope of S_i *vs.* Gly_0, from which p_{Gly} was determined using Eq. 7. The best-fit permeabilities were $2.3 \pm 0.23 \times 10^{-6}$ *vs.* $0.92 \pm 0.086 \times 10^{-6}$ cm sec^{-1} (MIP *vs.* Control) assuming the oocyte is a smooth sphere with $A_M = 0.045$ cm^2. If the oocyte membrane area including villi is used to normalize permeabilities (Kushmerick et al., 1995; Zampighi et al., 1995) the values would be about 8 times smaller. The permeability of MIP was specific; expression of MIP caused no detectable change in the permeability of urea, inositol, glucose, reduced glutathione or sorbitol (Kushmerick et al., 1995).

Single-Channel Glycerol Permeability

To determine the single-channel permeability, one must know the number of channels expressed in the oocyte plasma membrane. Quantitative immunoblotting of total oocyte homogenate (Kushmerick et al., 1995) indicated expression of $2.5 \pm 0.5 \times 10^{12}$ copies of MIP per oocyte. In the membrane MIP forms a tetramer, thus there are on the order of 6.3×10^{11} channels per oocyte. However, some significant fraction of these are in intracellular membranes, so this is an upper limit on the number of plasma membrane channels. A better estimate can be obtained based on the total water permeability per oocyte due to MIP and the single channel water permeability of MIP. In these oocytes, MIP induces an increase in total osmotic water permeability (P_{H2O}) of $1.2 \pm 0.04 \times 10^{-4}$ cm^3 sec^{-1} (calculated as described in Materials and Methods). Zampighi et al. (1995) estimate the single-channel water permeability of a MIP tetramer is approximately 6×10^{-16} cm^3 sec^{-1}, which implies our oocytes

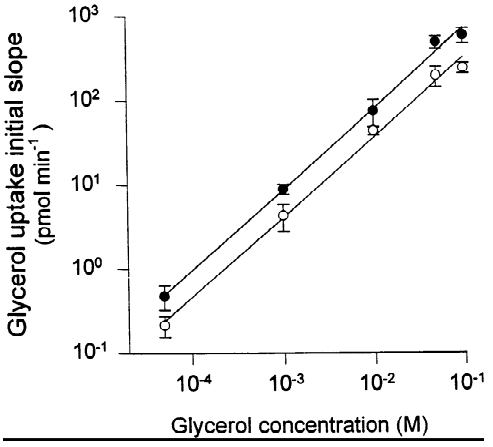

Fig. 4. Concentration dependence of p_{Gly}. The initial slope of glycerol uptake was measured as a function of glycerol concentration in oocytes expressing MIP (●) or control oocytes (○). Data points are means of 5–6 oocytes. Error bars are standard deviations. In both cases, the relationship was linear indicating p_{Gly} is independent of glycerol concentration over this range.

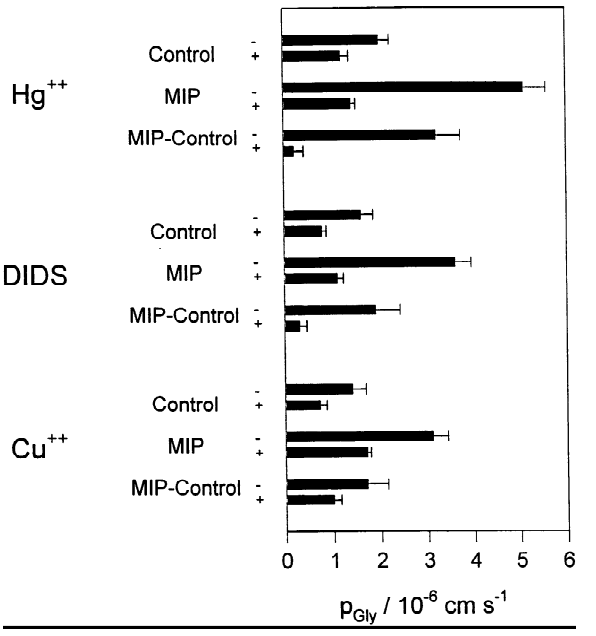

Fig. 5. Inhibition of p_{Gly}. p_{Gly} of oocytes with or without MIP, and the difference (MIP-Control) was determined in normal Ringers solution (−) or in Ringers plus the indicated inhibitor (+) from the initial slope of glycerol uptake using Eq. 7. Gly_o was 5 mM. Inhibitors: Hg^{++}: 1 mM $HgCl_2$; DIDS: 200 μM diisothiocyanodisulfonic stilbene; Cu^{++}: 200 mM $CuCl_2$. Bars are means of 5–6 oocytes. Error bars are standard deviations. Error bars for the difference, MIP-Control were determined from the variance in each as $(Var_{MIP} + Var_{Control})^{1/2}$.

are expressing 2×10^{11} channels (tetramers) in the plasma membrane. This is consistent with our upper limit of 6.3×10^{11} total channels based on immunoblotting data. The total glycerol permeability per oocyte is $P_{Gly} = p_{Gly}A_M$ (cm^3 sec^{-1}). The MIP-induced increase in total glycerol permeability per oocyte is therefore 0.62×10^{-7} cm^3 sec^{-1}. Dividing by the number of channels gives the single-channel glycerol permeability of MIP at approximately 3.1×10^{-19} cm^3 sec^{-1}. Though this number is obviously uncertain due to the difficulty in estimating the number of MIP in the plasma membrane, it nevertheless demonstrates that MIP is three orders of magnitude less permeable to glycerol than water. This suggests glycerol and MIP have different pathways through the MIP tetramer.

Inhibition of p_{Gly}

To demonstrate that the increase in p_{Gly} seen in Fig. 4 is directly due to transport properties of MIP, we looked for a specific blocking agent. Since 1.0 mM Hg^{++} and 200 μM DIDS block glycerol transport by other members of the MIP superfamily (Maurel et al., 1994; Ishibashi et al., 1994; Ma et al., 1994), and 0.1 mM Cu^{++} blocks protein-mediated glycerol transport in erythrocytes (Carlsen & Wieth, 1976), we examined the effect of these three agents on the p_{Gly} of MIP.

Figure 5 shows the p_{Gly} of oocytes in normal Ringer solution or in the presence of Hg^{++}, DIDS, or Cu^{++}. The component of p_{Gly} attributable to MIP (Fig. 5, bars labeled ''MIP-Control'') was determined as p_{Gly} (oocytes expressing MIP)—p_{Gly} (Control oocytes), either in normal solution or in the presence of inhibitor. The p_{Gly} of MIP was inhibited by all three agents, with potencies 1 mM Hg^{++} > 200 mM DIDS > 0.1 mM Cu^{++}. The inhibition of glycerol permeability by 1 mM Hg^{++} is in contrast to the observation that Hg^{++} does not appear to inhibit the water permeability of MIP (Kushmerick et al., 1995). This suggests glycerol and water may follow separate paths through the MIP channel.

These experiments were performed at $Gly_o = 5$ mM, which is 500 times the measured K_M for glycerol kinase. The influx of glycerol under these conditions ($= P_{Gly} \times Gly_o$) was therefore on the order of 10 pmol min^{-1}. This is ~100 times greater than the maximum rate of glycerol phosphorylation in the oocytes. Therefore, it is likely that the inhibition of glycerol uptake by these agents is due solely to an effect on permeability and is uncontaminated by any effects these agents may have on glycerol metabolism.

Temperature Sensitivity of p_{Gly}

The temperature sensitivity of the p_{Gly} of MIP provides clues about the mechanism of transport. If MIP forms a water-filled pore, the Q_{10} of p_{Gly} should be ~1.2, which is the Q_{10} for the viscosity of water at room temperature (Finkelstein, 1987). In contrast, the Q_{10} for glycerol per-

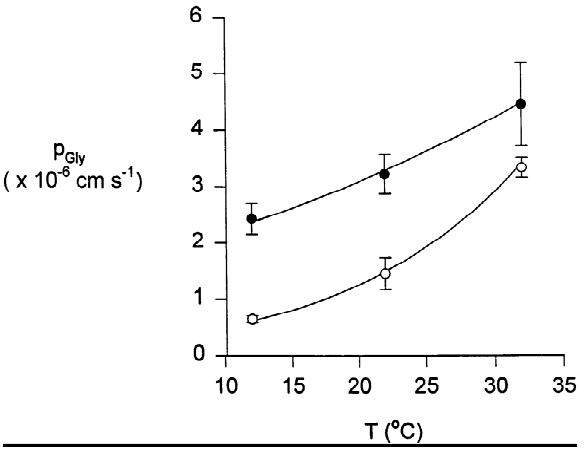

Fig. 6. Temperature dependence of p_{Gly}.p_{Gly} of oocytes with MIP (●) or controls (○) was determined in Ringers solution at the indicated temperatures from the initial slope of glycerol uptake using Eq. 7. Gly_o was 5 mM. Data points are the means from 4–6 oocytes, error bars are standard deviations. The smooth lines are best-fit theory curves as described in Materials and Methods.

meation though the oocyte plasma membrane lipid bilayer is expected to be more than twice this value. This is due, roughly in equal parts, to the enthalpy of partitioning of glycerol between water and the lipid, and the temperature sensitivity of non-Stokesian diffusion in the polymer environment of the bilayer hydrocarbon core (Stein, 1986). Consistent with this, the glycerol permeability of phosphatidyl choline/cholesterol liposomes has Q_{10} values ranging from 2.4–3.4 depending on the membrane composition (calculated from data in Van Zoelen et al., 1978; De Gier et al., 1971). The Q_{10} of glycerol transport via a solute carrier or pump should be relatively high as such a mechanism involves changes in the transporter configuration within the plasma membrane.

Figure 6 shows the temperature dependence of p_{Gly} of oocytes expressing MIP and control oocytes. In these experiments, Gly_o was 5 mM. p_{Gly} in control oocytes had a Q_{10} of 2.4. Together with the fact that the p_{Gly} of control oocytes was similar to that reported for the basal p_{Gly} of the red cell plasma membrane (10), and is independent of concentration (*cf.* Fig. 4), this suggests that in control oocytes, glycerol permeation occurs by diffusion through the plasma membrane. Glycerol permeability in oocyte expressing MIP had a significantly reduced Q_{10} relative to controls (1.4 *vs.* 2.4), suggesting MIP introduces a qualitatively different pathway, one more similar to diffusion in water than through a lipid bilayer.

Discussion

In a previous paper, we reported expression of MIP had two effects on glycerol uptake in oocytes: it increased the initial slope, consistent with an increase in permeability, and it added a late component of uptake, consistent with either active transport or enhanced trapping of glycerol as an impermeant form (Kushmerick et al., 1995). In the present paper, we demonstrate accumulation of metabolic products of glycerol, primarily glycerol-3-phosphate (G3P) and phospholipids, account for the late component of glycerol uptake and show MIP exerts its effect on this component by stimulating glycerol kinase (GK).

We developed a method to study GK activity as a function of the concentration of free intracellular glycerol in intact oocytes expressing MIP. The reactions we assumed occur are given as Eq. 1. This model assumes glycerol uptake is passive, and that intracellular glycerol is phosphorylated by glycerol kinase, thus trapping it and allowing total ^{3}H-glycerol radioactivity to accumulate beyond equilibrium with the bath. Analysis of this scheme yielded an expression for the intracellular free glycerol concentration (Eq. 6), which was used to determine the kinetic parameters of glycerol kinase activity (K_M and k_pGK_T).

For simplicity, the only component of the final slope listed in Eq. 1 is G3P. In these experiments, we measure total oocyte radioactivity, which includes glycerol and all of its impermeant metabolites. G3P may enter the glycolytic pathway and some of the radioactivity from glycerol may exit the cell as ^{3}H-H_2O. In general, we may express the final slope as

$$GKC_{ss} \xrightarrow{k_p} \boxed{\Sigma GK_n} \xrightarrow{k_w} H_2O$$

where the GP_n are the impermeant products that accumulate in the cell, and k_w is the effective rate constant for the formation of ^{3}H-H_2O from its precursor(s) which we will refer to as GP_N. The final slope is therefore given by

$$\frac{d\,\Sigma GP_n}{dt} = k_p\,GKC_{ss} - k_w GP_N \tag{8}$$

If $k_w = 0$ then the final slope is exactly k_pGKC_{ss}, as assumed in the analysis above. If $k_w \neq 0$, then accumulation will approach a steady-state condition given by

$$\frac{d\,\Sigma GP_n}{dt} = 0$$
$$k_p\,GKC_{ss} = k_w\,GP_N \tag{9}$$

Since in our data, uptake is linear in the time frame (200 min < t < 1420 min), we conclude the term k_wGP_N in Eq. 8 is small, so that, as above,

$$\frac{d\,\Sigma GP_n}{dt} \simeq k_pGKC_{ss} \tag{10}$$

The model explains our observations. Phosphorylation is the first intracellular step in processing glycerol. Since the available data suggest higher organisms lack glycerol-3-phosphatase activity (Lackner et al., 1984), this reaction is essentially irreversible and sets the rate of glycerol incorporation into the several pathways.

We have concluded expression of MIP increased the maximum rate of glycerol phosphorylation by oocytes, k_pGK_T, without changing the apparent affinity for glycerol, K_M. Our method does not allow us to determine which of the two variables (k_p or GK_T) increased. An increase in GK_T would presumably involve induction of *GK* synthesis, whereas an increase in k_p suggests allosteric regulation of *GK* by MIP. The bacterial glycerol facilitator, glpF, increases glycerol kinase activity via a direct interaction (Voegele et al., 1993). MIP may also interact directly with glycerol kinase, allosterically regulating the enzyme. If true, one should be able to colocalize MIP and *GK* using chemical crosslinkers. Unfortunately, while theoretically feasible, this technique has not been successful in demonstrating the physical connection between glpF and glycerol kinase (Voegele et al., 1993).

We considered alternate explanations for the effect of MIP on glycerol accumulation. G3P could inhibit *GK* activity, either by mass action or by enzyme inhibition, and MIP could indirectly enhance *GK* by enhancing a reaction that decreases the level of G3P. However, under physiologic conditions, glycerol phosphorylation is essentially irreversible ($\Delta G < -9$ kCal mol^{-1}). Competitive inhibition of *GK* by G3P occurs with a K_i on the order of 1 mM (Lin, 1977) and therefore is unlikely to be involved in the effect of MIP since we saw increases in *GK* activity when $Gly_{i\text{-}ss}$ (and therefore G3P) are on the order of 10 μM. Changes in ATP levels due to MIP are also unlikely to account for its affect on *GK* activity, because the dissociation constant of *GK* for ATP is 50–100 μM whereas cellular [ATP] is typically 5–10 mM, and the oocyte is an energy-rich cell. MIP could inhibit dephosphorylation of G3P, thus allowing it to rise to a higher steady-state level. However, although a specific glycerol-3-phosphatase exists in yeast and certain protozoa, the data available suggest it is not detectable in higher organisms (Lackner et al., 1984).

Induction of *GK* synthesis occurs in yeast grown in the presence of glycerol, with intracellular glycerol itself the inducing agent (Gancedo, Gancedo & Sols, 1968). However, glycerol-induced glycerol kinase can not explain the data in Fig. 4. If Gly_i determined the final slope, then both control oocytes and oocytes expressing MIP would have the same final slope at high enough values of Gly_o. Since Fig. 4 shows this is not the case, this mechanism is unlikely.

We conclude the most likely mechanism of MIP increasing glycerol phosphorylation is also the simplest: the activity of glycerol kinase is increased in the presence of MIP.

Role of Glycerol in the Lens

Glycerol, glycerol kinase and glycerol-3-phosphate are all found in the fiber cell (Kuck, 1970), suggesting a role for glycerol in lens fiber cell metabolism or membrane synthesis. In human plasma, glycerol is present at 0.05–0.1 mM (Lin, 1977). Since the aqueous humor is formed partially as an ultrafiltrate of plasma (Cole, 1970) glycerol is probably present in the aqueous humor as well.

The phospholipid constituents of most cell membranes have half-lives on the order of hours (van den Bosch, 1980). Lens fiber cells lack the normal complement of reticula and lysosomes to synthesize and degrade their membranes, resulting in relatively low levels of membrane lipid synthesis. Nonetheless, lens lipids are subject to equal or greater oxidative damage than those of other cells and it seems unlikely they last for the life of the organism. Moreover, changes in lens membrane composition with age have been documented (Broekhuyse & Daemen, 1976), and glycerol-3-phosphate is a precursor of phospholipid synthesis. Thus one role of MIP in the lens may be to facilitate the uptake of glycerol from the aqueous humor, and in conjunction with glycerol kinase, catalyze its subsequent incorporation into lipid or metabolism.

Expression of MIP increased the oocyte glycerol permeability by a factor of 2–3, however in the lens the effect could be greater. The permeability of the lens membrane lipid is expected to be low, due to the high levels of long-chained saturated phospholipids, cholesterol, and sphingomyelin (Zelenka, 1984), all of which reduce diffusion through the hydrocarbon core, which is the rate-limiting step in permeation through lipid bilayers (Shinitzky, 1984). Moreover, the density of MIP in the lens is extremely high, especially in the localized patches of crystalline arrays described by Zampighi et al. (1989). The combination of low background permeability and high density could lead to MIP having a larger impact on permeability in the lens than in the oocyte.

Comparison with other Members of the Superfamily

In addition to increasing glycerol phosphorylation, MIP increased the glycerol permeability, p_{Gly}, of oocytes 2.5-fold (Fig. 1*B*, 3*A*, 4–6). p_{Gly} due to MIP was inhibited by heavy metals and DIDS, and had a low temperature sensitivity. In this regard, MIP acts as a channel with biophysical properties similar to other members of its superfamily.

Three other members of the MIP superfamily reported to be glycerol facilitators are glpF, FSP1 and

Table 3. Percent amino acid sequence identity/similarity between members of the MIP superfamily reported to transport glycerol

	glpF	FSP1	AQP3/GLIP
Frog lens MIP	29/57	30/57	31/58
AQP3/GLIP	40/62	32/60	
FSP1	33/60		

glpF: *E. coli* glycerol facilitator. FPS1: Yeast Fermentable Sugar Protein 1, AQP3/GLIP: Aquaporin 3/Glycerol Intrinsic Protein of mammalian kidney. Sequences were compared using the GAP program (Genetics Computer Group, Madison, WI).

AQP3 (also known as GLIP). glpF and FPS1 are bacterial glycerol facilitators in *E. coli* and yeast respectively (Sweet et al., 1990; Van Aelst et al., 1991), while AQP3/GLIP is an Aquaporin in the collecting duct of mammalian kidney (Ishibashi et al., 1994; Echevarria et al., 1994; Ma et al., 1994). The percent amino acid identity/similarity among each of these proteins and MIP is given in Table 3.

When expressed in *Xenopus* oocytes, the *E. coli* glycerol facilitator, GlpF, increased p_{Gly} 5-fold, exhibited a lack of concentration dependence and was inhibited by 1 mM $HgCl_2$ similar to MIP (Maurel et al., 1994). These authors measured p_{Gly} at $Gly_o = 100$ mM. Under these conditions, glycerol phosphorylation is negligible compared to glycerol influx. Thus it is not known whether glpF activates glycerol kinase in oocytes as it does in *E. coli* (Voegele et al., 1993).

FPS1 is a yeast glycerol facilitator that gates closed in response to hypertonic shock, and is therefore believed to be involved in glycerol-mediated osmoregulation. FPS1 also increases glycerol production in yeast, suggesting FPS1 also plays some role in glycerol metabolism (Luyten et al., 1995). No data are available for the metal sensitivity or temperature dependence of FPS1, nor has anyone reported expression of FPS1 in oocytes.

AQP3 (or GLIP) increased P_{Gly} when expressed in oocytes (Ishibashi et al., 1994; Ma et al., 1994). There is, however, disagreement regarding its selectivity and heavy metal sensitivity; some reports indicate it transported urea (Ishibashi et al., 1994; Echevarria et al., 1994) and was inhibited by Hg^{++} (Ishibashi et al., 1994) while other reports suggest it had no urea permeability and its glycerol permeability was inhibited by DIDS but not Hg (Ma et al., 1994). Lens MIP transports glycerol and not urea, and is inhibited by both $HgCl_2$ and DIDS. Thus in some respects MIP behaves similarly to AQP3 (GLIP), however confirmation of this will have to wait until the discrepancies described above are settled.

In conclusion, we have shown that in addition to acting as a glycerol channel, MIP also affects glycerol metabolism by activating glycerol kinase. There is now evidence that three members of the MIP superfamily, glpF (Voegele et al., 1993), FPS1 (Luyten et al., 1995) and lens MIP (this paper), are involved in metabolism as well as transport, a fact that may help in understanding the physiological role of other members of the superfamily.

We are grateful to Drs. Mario Rebecchi, Nada Abumrad, Raafat El-Maghrabi and Howard C. Haspel for helpful discussions and criticisms. This work was supported by National Institutes of Health grant EY06391 from the NEI.

References

Agre, P., Preston, G.M., Smith, B.L., Jung, J.D., Raina, S., Moon, C., Guggino, W.B., Nielsen, S. 1993. Aquaporin CHIP: the archetypal molecular water channel. *Am. J. Physiol.* **265:**F463–476

Austin, L.R., Rice, S.J., Baldo, G.J., Lange, A.J., Haspel, H.C., Mathias, R.T. 1990. The cDNA sequence encoding the maor intrinsic protein of frog lens. *Gene.* **124:**303–304

Baker, M.E., Saier, Jr., M.H. 1990. A common ancestor for bovine lens fiber major intrinsic protein, soybean nodulin-26 protein, and *E. coli* glycerol facilitator. *Cell* **60:**185–186

Bergmeyer, H.U. 1984. *In:* Methods of Enzymatic Analysis, 3rd. Edition. H.U. Bergmeyer, editor, Vol VI, p 526. VCH, Deerfield Beach, FL

Beyer, E.C., Paul, D.L., Goodenough, D.A. 1987. Connexin43: a protein from rat heart homologous to a gap junction protein from liver. *J. Cell. Biol.* **105:**2621–2629

Broekhuyse, R.M., Daemen, F.J.M. 1976. The Eye. *In:* Lipid Metabolism in Mammals. F. Snyder, editor. pp. 145–188. Plenum Press, New York, NY

Broekhuyse, R.M., Kuhlmann, E.D., Stols, A.L. 1976. Lens membranes II. Isolation and characterization of the main intrinsic polypeptide (MIP) of bovine lens fiber membranes. *Exp. Eye Res.* **23:**365–371

Carlsen, A., Wieth, J.O. 1976. Glycerol transport in human red cells. *Acta Physiologica Scandinavica.* **97:**501–513

Cole, D.F. 1970. Aqueous and Ciliary Bodies. *In:* Biochemistry of the Eye. C.N. Graymore, editor. pp. 105–181. Academic Press, New York, NY

De Gier, J., Mandersloot, J.G., Hupkes, J.V., McElhaney, R.N., and Van Beek, W.P. 1971. On the mechanism of non-electrolyte permeation through lipid bilayers and through biomembranes. *Biochim. Biophys. Acta.* **233:**610–618

Echevarria, M., Windhager, E.E., Tate, S.S., Frind, G. 1994. Cloning and expression of AQP3, a water channel from the medullary collecting duct of rat kidney. *Proc. Natl. Acad. Sci. USA* **91:**10997–11001

Ehring, G.R., Zampighi, G., Horwitz, J., Bok, D., Hall, J.E. 1990. Properties of channels reconstituted from the major intrinsic protein of lens fiber membranes. *J. Gen. Physiol.* **96:**631–664

Finkelstein, A. 1987. Water Movement Through Lipid Bilayers, Pores, and Plasma Membranes Theory and Reality. *In:* Distinguished Lecture Series of the Society of General Physiologists. Volume 4. pp. 158–159. John Wiley & Sons, New York, NY

Gancedo, C., Gancedo, J.M., Sols, A. 1968. Glycerol metabolism in yeasts. Pathways of utilization and production. *Eur. J. Biochem.* **5:**165–172

Girsch, S.J., Peracchia, C. 1985. Lens cell-to-cell channel protein: I. Self-assembly into liposomes and permeability regulation by calmodulin. *J. Membrane Biol.* **83:**217–225

Gorin, M.B., Yancey, S.B., Cline, J., Revel, J.P., Horwitz, J. 1984. The

major intrinsic protein (MIP) of the bovine lens fiber membrane: characterization and structure based on cDNA cloning. *Cell* **39:**49–59

Ishibashi, K., Sasaki, S., Fushimi, K., Uchida, S., Kuwahara, M., Saito, H., Furukawa, T., Nakajima, K., Yamaguchi, Y., Gojobori, T., Marumo, F. 1994. Molecular cloning and expression of a member of the aquaporin family with permeability to glycerol and urea in addition to water expressed at the basolateral membrane of kidney collecting duct cells. *Proc. Natl. Acad. Sci. USA* **91:**6269–6273

Kates, M. 1986. *In:* Techniques of Lipidology. Laboratory techniques in biochemistry and molecular biology. R.H. Burdon and P.H. van Knippenberg, editors. Vol 3, pt 2, pp. 232–254. Elsevier, New York, NY

Klaidman, L.K., Leung, A.C., Adams Jr., J.D. 1995. High-performance liquid chromatography analysis of oxidized and reduced pyridine dinucleotides in specific brain regions. *Anal. Biochem.* **228:**312–317

Kuck, J.F.R. 1970. Chemical Constituents of the Lens. *In:* Biochemistry of the Eye. C.N. Graymore, editor. pp. 183–260. Academic Press, New York, NY

Kushmerick, C., Rice, S.J., Baldo, G.J., Haspel, H.C., Mathias, R.T. 1995. Ion, water and neutral solute transport in *Xenopus* oocytes expressing frog lens MIP. *Exp. Eye Res.* **61:**351–362

Lackner, R., Challiss, R.A., West, D., Newsholme, E.A. 1984. A problem in the radiochemical assay of glucose-6-phosphatase in muscle. *Biochem. J.* **218:**649–651

Lin, E.C. 1977. Glycerol utilization and its regulation in mammals. *Ann. Rev. Biochem.* **46:**765–795

Luyten, K., Albertyn, J., Skibbe, W.F., Prior, B.A., Ramos, J., Thevelein, J.M., Hohmann, S. 1995. Fps1, a yeast member of the MIP family of channel proteins, is a facilitator for glycerol uptake and efflux and is inactive under osmotic stress. *EMBO J.* **14:**1360–1371

Ma, T., Frigeri, A., Hasegawa, H., Verkman, A.S. 1994. Cloning of a water channel homolog expressed in brain meningeal cells and kidney collecting duct that functions as a stilbene-sensitive glycerol transporter. *J. Biol. Chem.* **269:**21845–21849

Mathias, R.T., Rae, J.L., Ebihara, L., McCarthy, R.T. 1985. The localization of transport properties in the frog lens. *Biophys. J.* **48:**423–434

Maurel, C., Reizer, J., Schroeder, J.I., Chrispeels, M.J., Saier Jr., M.H. 1994. Functional characterization of the *Escherichia coli* glycerol facilitator, GlpF, in *Xenopus* oocytes. *J. Biol. Chem.* **269:**11869–11872

Mulders, S.M., Preston, G.M., Deen, P.M., Guggino, W.B., van Os, C.H., Agre, P. 1995. Water channel properties of major intrinsic protein of lens. *J. Biol. Chem.* **270:**9010–9016

Shiels, A., Bassnett, S. 1996. Mutations in the founder of the MIP gene family underlie cataract development in the mouse. *Nature Genetics.* **12:**212–215

Shinitzky, M. 1984. Membrane fluidity and cellular functions. *In:* Physiology of Membrane Fluidity, M. Shinitzky, editor. Vol. 1, pp. 2–52. CRC Press, Boca Raton, FL

Stein, W.D. 1986. Transport and Diffusion across Cell Membranes. pp. 69–112. Academic Press, Orlando, FL

Sweet, G., Gandor, C., Voegele, R., Wittekindt, N., Beuerle, J., Truniger, V., Lin, E.C., Boos, W. 1990. Glycerol facilitator of *Escherichia coli:* cloning of glpF and identification of the glpF product. *J. Bacteriol.* **172:**424–430

Swenson, K.I., Jordan, J.R., Beyer, E.C., Paul, D.L. 1989. Formation of gap junctions by expression of connexins in *Xenopus* oocyte pairs. *Cell* **57:**145–155

Van Aelst, L., Hohmann, S., Zimmermann, K.F., Jans, A.W., Thevelein, J.M. 1991. A yeast homologue of the bovine lens fibre MIP gene family complements the growth defect of a *Saccharomyces cerevisiae* mutant on fermentable sugars but not its defect in glucose-induced RAS-mediated cAMP signalling. *EMBO J.* **10:**2095–2104

van den Bosch, H. 1980. Intracellular phospholipases A. *Biochim. Biophys. Acta.* **604:**191–246

Van Zoelen, E.J., Henriques de Jesus, C., de Jonge, E., Mulder, M., Blok, M.C., de Gier, J. 1978. Non-electrolyte permeability as a tool for studying membrane fluidity. *Biochim. Biophys. Acta.* **511:**335–347

Voegele, R.T., Sweet, G.D., Boos, W. 1993. Glycerol kinase of *Escherichia coli* is activated by interaction with the glycerol facilitator. *J. Bacteriol.* **175:**1087–1084

Whitesell, R.R., Abumrad, M.K., Powers, A.C., Regen, D.M., Le, C., Beechem, C.M., May, J.M., Abumrad, N. 1993. Coupling of glucose transport and phosphorylation in *Xenopus* oocytes and cultured cells: determination of the rate-limiting step. *J. Cell. Physiol.* **157:**509–518

Zampighi, G.A., Hall, J.E., Ehring, G.R., Simon, S.A. 1989. The structural organization and protein composition of lens fiber junctions. *J. Cell Biol.* **108:**2255–2275

Zampighi, G.A., Kreman, M., Boorer, K.J., Loo, D.D., Bezanilla, F., Chandy, G., Hall, J.E., Wright, E.M. 1995. A method for determining the unitary functional capacity of cloned channels and transporters expressed in *Xenopus laevis* oocytes. *J. Membrane Biol.* **148:**65–78

Zelenka, P.S. 1984. Lens lipids. *Curr. Eye Res.* **3:**1337–1359